machines

MDPI

Article

Identification of Heat Transfer Parameters for Gravity Sand Casting Simulations

Alberto Vergnano [1,*], Pietro Facondini [2], Nicolò Morselli [1], Paolo Veronesi [1] and Francesco Leali [1]

[1] Enzo Ferrari Department of Engineering, University of Modena and Reggio Emilia, Via P. Vivarelli 10, 41125 Modena, Italy; nicolo.morselli@unimore.it (N.M.); paolo.veronesi@unimore.it (P.V.); francesco.leali@unimore.it (F.L.)
[2] Fonderia Morri, Via A. Manzoni 7, 47853 Cerasolo, Italy; tecnico@fonderiamorri.it
* Correspondence: alberto.vergnano@unimore.it

Abstract: Gravity sand casting simulations require accurate modelling of heat transfer phenomena to reliably evaluate the expected quality of the produced parts. Average model parameters can be easily retrieved from a validated database. However, these parameters are highly dependent on the specific sand used and the actual forming process in the foundry. Furthermore, the heat transfer from the solidifying alloy to the mould surfaces is not precisely known, so simulation models usually use typical values for overall heat transfer coefficients. Most research works investigate individual parameters, whereas heat transfer phenomena largely arise from their interaction together. Therefore, the present work describes a combined experimental and computational method based on genetic algorithm techniques for determining the most important parameters for heat transfer in a sand mould. The experiments examine both virgin and reused sand, as these are alternatively used in the foundry for mould forming. The density, thermal conductivity, and specific heat capacity of the different sands are identified, along with heat transfer coefficients. The counterproof simulations demonstrate that the standard parameters are quite reliable for virgin sand. However, in the case of reused sand, the identified parameters lead to more reliable results.

Keywords: gravity sand casting; thermal conductivity; volumetric heat capacity; heat transfer coefficient; parameter identification; genetic algorithms; reused sand

check for updates

Citation: Vergnano, A.; Facondini, P.; Morselli, N.; Veronesi, P.; Leali, F. Identification of Heat Transfer Parameters for Gravity Sand Casting Simulations. *Machines* **2024**, *12*, 414. https://doi.org/10.3390/machines12060414

Academic Editor: Angelos P. Markopoulos

Received: 23 May 2024
Revised: 11 June 2024
Accepted: 13 June 2024
Published: 17 June 2024

1. Introduction

Gravity Sand Casting (GSC) involves pouring molten metal into a sand mould to produce a part with intricate shapes. GSC simulations are fundamental to designing a mould capable of delivering specified quality levels [1,2], thus avoiding expensive trial and error in the foundry. Heat transfer plays a pivotal role in these simulations as it leads to the progressive solidification of the casting while maintaining a prolonged fluid connection with the feeders to compensate for its volume shrinkage during solidification. Therefore, identifying heat transfer parameters is essential to optimising the mould equipment and process parameters.

Different sands used for forming the mould exhibit specific thermal properties, significantly influencing heat transfer rates. Generally, the heat removal rate of a sand mould is lower than that of a permanent one manufactured from steel due to its lower volumetric heat capacity and thermal conductivity [3]. The volumetric heat capacity is lowered in direct proportion to the volume fraction of the pores and can be measured via differential scanning calorimetry. Thermal conductivity is also significantly reduced by the pores, as low air thermal conductivity increases overall thermal resistance. Thermal conductivity can be calculated from the density, specific heat capacity, and thermal diffusivity, measured via the flash diffusivity method [4,5]. Recent works derive conductivity by monitoring temperatures in dynamic conditions through high-resolution infrared thermography [6]. Advances in sensing technologies have enabled in situ measurements of thermal conductivity [7].

Experiments on these thermal properties have shown some positive correlation with density, but also some deviations. For instance, non-spherical pores worsen thermal conductivity more than spherical ones, and variations in grain size can have more significant effects than variations in pore volume fractions. The crystallographic structure of the sand and additives also has similar effects. The effective thermal properties of porous materials are complex to determine; therefore, the literature describes several alternative predictive models [8]. Some of these are based on a large dataset of thermal conductivity measurements or require many inputs to deliver the resulting parameters [9]. These techniques offer fundamental insights into the bulk thermal conductivity of the material; however, they may not capture the complex and dynamic nature of heat transfer in GSC processes.

In fact, thermal dynamics through the sand mould are further complicated by other physics phenomena. Hot air is vented from the cavities through the sand pores [10]. The gases generated from the burned binder of the sand must also be continuously vented, but this heats up the neighbouring sand. Determining the heat flux from the alloy to the sand often involves experimental measurements or numerical simulations [11], as it depends on various factors such as contact pressure, surface finishing, sand grain dimensions, coating thickness, and deformation of the casting, which can be difficult to model analytically. In GSC simulations, this heat flux is modelled as an overall Heat Transfer Coefficient (HTC), which is the proportionality constant between heat flux and temperature difference between the contacting surfaces per unit area [12,13]. The HTC between casting and mould surfaces is not precisely known, and the simulations rely on typical HTC values available in the software database. If the reliability of the results must be improved, HTCs are identified with experimental and inverse optimisation procedures [14,15]. The literature on identifying heat transfer coefficients in GSC demonstrates a diverse range of approaches, none of which is easily usable for setting up simulation models. Furthermore, most methods use specimens expressly produced for the experiments. By contrast, the heat transfer properties of sand heavily depend on the actual forming process in the foundry. In foundries, sand is conveniently reused several times, changing its physical and thermal properties. Hence, a gap exists in the literature as the variation in properties during actual use and reuse is not studied.

The present work describes a combined experimental and computational method for identifying the most important parameters for heat transfer through a sand mould. This paper is organised as follows: Section 2 introduces the GSC equipment used in the experiments and the identification technique through inverse optimisation. Section 3 presents a case study on identifying the thermal parameters of virgin and reused sand, and Section 4 provides concluding remarks.

2. Technique and Equipment for Parameter Identification of Sand Moulds

The present research follows the workflow shown in Figure 1. It consists of four main phases that are further divided into activities carried out through simulations in the left column and experimental activities on the right. Note that parameter identification through inverse optimisation is carried out in two steps: the first identifies sand properties, while the second identifies heat transfer from the Al alloy to the mould. The properties of the sand are identified in the first step, since the heat resistance due to the solid mould is much higher than the resistance at the alloy-mould interface. This two-step identification is necessary to split the number of parameters in two, thus converging the algorithm towards an optimised result.

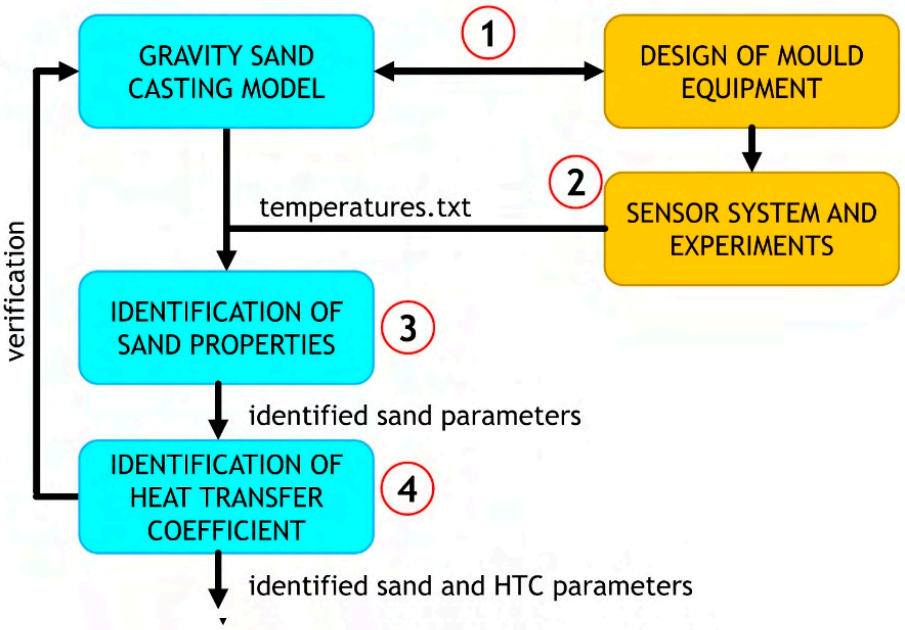

Figure 1. Workflow for the identification of heat transfer parameters for GSC simulations.
Figure 1. Workflow for the identification of heat transfer parameters for GSC simulations.

2.1. Design of Mould Equipment and Experiments

The first phase is to design an experiment that reduces the influence of uncontrollable factors on heat transfer phenomena. The real experiment must also be modelled in a sand-casting simulation. In the present research, the model was designed using Magmasoft 6.0 software [16]. Figure 2 shows the CAD model for the simulation, which includes transparent steel frames, green sand moulds, grey cavities, and an orange inlet. The three thermocouples, T1, T2, and T3, represented by blue dots, are 10 mm, 25 mm, and 40 mm distant from the casting, respectively. The casting has an approximate diameter of 100 mm and a length of 250 mm. Considering the casting system, the total weight of the poured alloy is approximately 4.2 kg. Note that contact between the alloy and air is reduced to a minimum to avoid heat exchange in a medium that varies from day to day.

The first phase is to design an experiment that reduces the influence of uncontrollable factors on heat transfer phenomena. The real experiment must also be modelled in a sand-casting simulation. In the present research, the model was designed using Magmasoft 6.0 software [16]. Figure 2 shows the CAD model for the simulation, which includes transparent steel frames, green sand moulds, grey cavities, and an orange inlet. The three thermocouples, T1, T2, and T3, represented by blue dots, are 10 mm, 25 mm, and 40 mm distant from the casting, respectively. The casting has an approximate diameter of 100 mm and a length of 250 mm. Considering the casting system, the total weight of the poured alloy is approximately 4.2 kg. Note that contact between the alloy and air is reduced to a minimum to avoid heat exchange in a medium that varies from day to day.

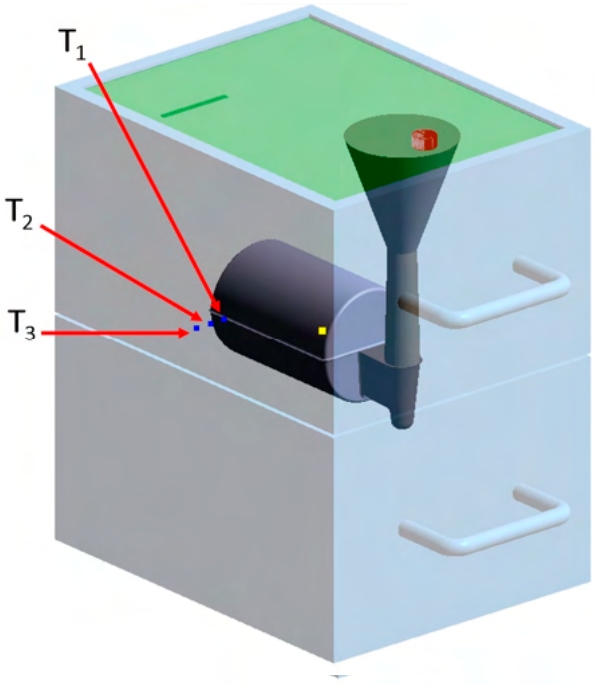

Figure 2. CAD model for the simulations.
Figure 2. CAD model for the simulations.

fully filled with more sand to create a flat surface at the parting plane between the lowe
and upper moulds.

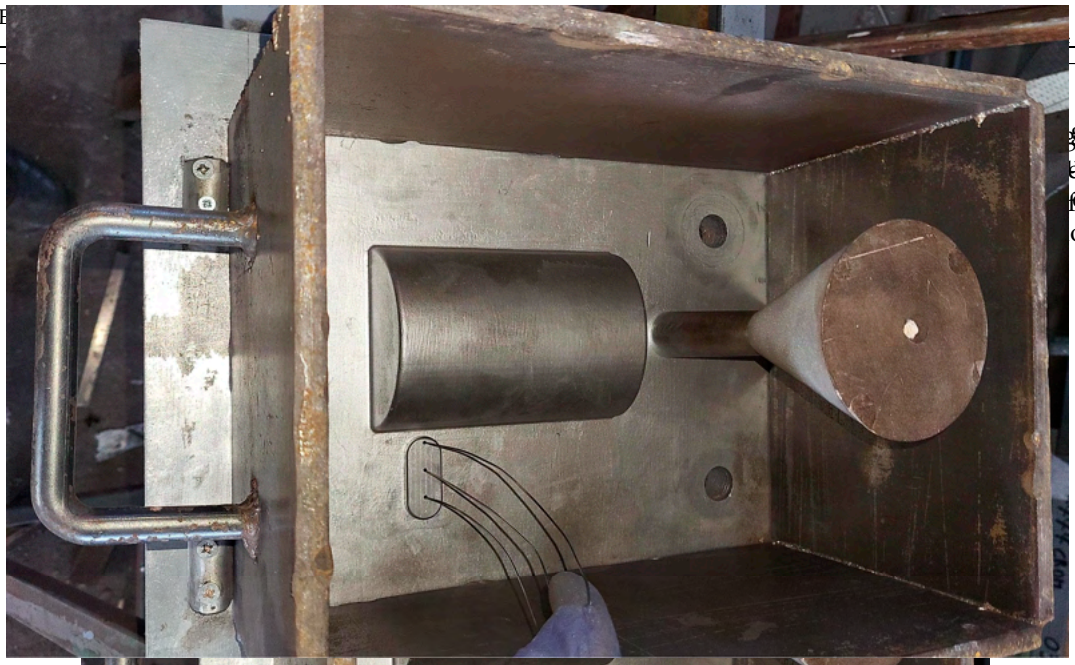

Figure 3. Forming equipment with an insert for retaining the thermocouple stems.

Model 01, shown in Figure 2, with three thermocouples simulated as points, was used
as a reference in preliminary evaluations. The protection of thermocouples in this experi
ment is still an open issue. Therefore, to simulate the experiment as accurately as possible
including perturbations due to thermocouples, several alternative models were examined,
each presenting distinct adjustments. These models are illustrated in Figure 4 and can b
described as follows:

(02) thermocouple stems are 1 mm in diameter;
(03) additional steel tubes protect thermocouple stems;
(04) protective steel tubes are closed at the tip;
(05) protective tubes are manufactured from copper;
(06) stems are protected with insulation sheets.

To evaluate the simplifications in the model and save on calculation time, model 0
in Figure 2 was simulated again as 07, considering only the solidification phase and no
the pouring phase.

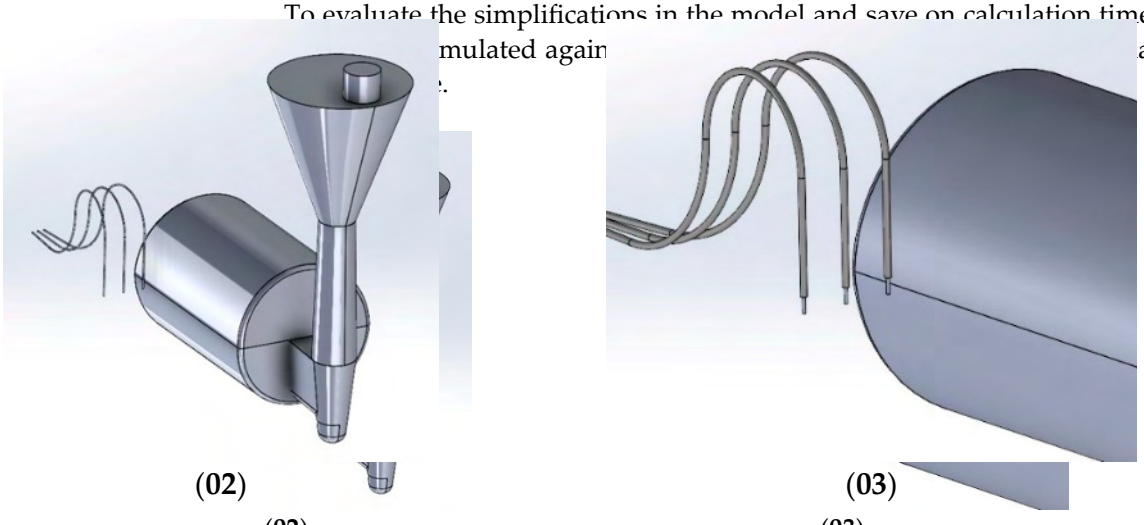

(**02**) (**03**)

Figure 4. *Cont.*

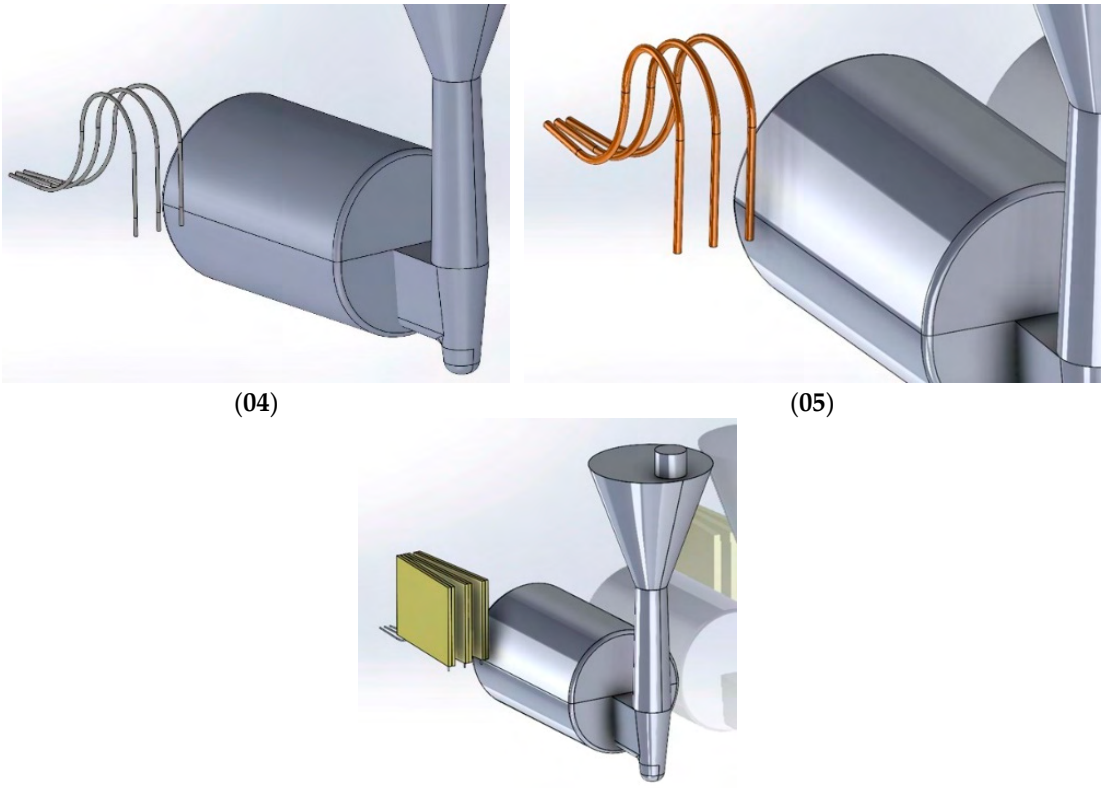

(**04**) (**05**)

(**06**)

Figure 4. Simulation models attempting to simulate experiment perturbation due to (**02**) thermocouple stems; (**03**) steel tubes protecting the thermocouple stems; (**04**) closed protective tubes; (**05**) copper protecting tubes; (**06**) stem protection with insulation sheets.

Figure 4. Simulation models attempting to simulate experiment perturbation due to (**02**) thermocouple stems; (**03**) steel tubes protecting the thermocouple stems; (**04**) closed protective tubes; (**05**) copper protecting tubes; (**06**) stem protection with insulation sheets.

To evaluate the simplifications in the model and save on calculation time, model 01 in Figure 2 was simulated again as 07, considering only the solidification phase and not the pouring phase.

In Magmasoft, the generation of the cartesian mesh is done automatically after setting its default, advanced, and coarsening parameters. The Multiple Parameter Sets method was used to achieve an optimal mesh concerning the specific simulation tasks and time. The mesh was created coarse with a default size of 5 mm equidistant in all directions for all materials to save calculation time, especially since the goal of this bulky casting is to provide heat in the experiment rather than delivering a quality casting. However, modelling the position of the thermocouple tips as precisely as possible is essential. Since the hot junction of thermocouples is comparable in size to the 1 mm diameter of their stem, the advanced mesh size was refined to 1 mm at the tip position to simulate temperature gradients. The number of coarsening loops was set to 3 and the coarsening threshold was set to 2, resulting in a number of Cartesian cells of 1,073,856 and a number of cavity cells of 27,542.

The simulations considered AlSi9Cu1Mg poured at 720 °C. The alloy properties, such as density, specific heat, thermal conductivity, and latent heat, are modelled as functions of temperature and dynamically integrated by Magmasoft 6.0 software. The steel frame was initially at 20 °C, and silica dry sand was at 20 °C. The thermocouple insulating stems are composed of MgO, and the protective tubes consist of steel or copper. The protective sheets are simulated with insulating properties similar to those of Monolite [17]. The thermal conductivity and specific heat capacity of the sand and the HTC between the alloy and the steel frame, and between the steel frames, were the standard functions of the Magmasoft database. These functions are described in detail in Sections 2.3 and 2.4. The HTC was also set constant at

800 W/m^{2}K between the two sand moulds, 800 W/m^{2}K between the sand and the steel frame, and 3500 W/m^{2}K between the steel frames.

Figure 5 shows the simulated curves for the three thermocouples for all 01–07 models, showing minimal differences between the reference model (01) and those attempting to simulate perturbations due to the thermocouples (02–06).

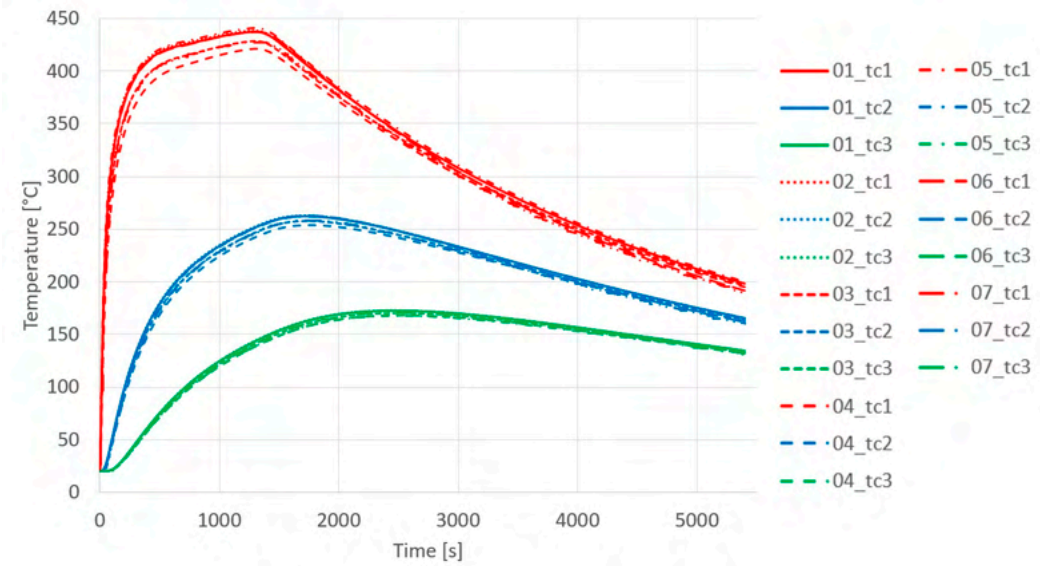

Figure 5. Simulated temperatures at the thermocouple tips for all preliminary simulations.

The heat transfer phenomenon is slow enough to equalise the temperature of the thermocouple stems with that of the surrounding sand, and the stems do not induce a significant thermal bridge. Furthermore, since the pouring phase requires less time than solidification, neglecting the former does not significantly influence the study results.

The simulation of the last 07 model took about 22 min to simulate on a workstation with four parallel cores running at 3.70 GHz and 64 GB of RAM. The other models needed 47–390 min and 295 min on average, demonstrating the possibility of further simplifying the simulation.

This first sensitivity analysis validates the choice of the simplified model 07, which considers only the solidification phase but not the pouring one, with the three thermocouples simulated as points, for use in the subsequent identification phases of the sand parameters.

2.2. Sensor System and Experiment

The temperatures were monitored via three 405-279 K-type mineral-insulated metal-sheathed thermocouples with 1 mm diameter and 1000 mm length from TC Direct (Hillside, IL, USA) [18]. They were connected with 818-432-KX-type extension cables, twisted, shielded, and PVC insulated, with 724-102 and 724-104 K-type miniature connectors. In the experiments, the thermocouple stems were protected with an insulating sheet, as shown in Figure 4 for model 06 and analysed in Figure 5. The thermocouples were connected to a TC-08 thermocouple data logger from Pico Technology (Saint Neots, UK) [19]. The thermocouples were calibrated together with the numbered connecting cables through a Fluke 9142 (Fluke, Everett, WA, USA) RTD dry-block temperature analyser equipped with a PT100 probe [20]. The thermocouples were calibrated to 0.1 °C [20]. Even though the experiment was specifically designed for the casting was carried out in a sand foundry facility, a normal production, including the sand, forming equipment, air environment, and steel alloy. Prior to pouring, the temperature of the alloy was measured through a high-temperature probe, while an infrared thermometer gun measured all the materials in the experiment. These temperatures were registered and used in the subsequent phase of inverse optimisation to initialise the simulation temperatures.

2.2. Sensor System and Experiment

The temperatures were monitored via three 405-279 K-type mineral-insulated metal-sheathed thermocouples with 1 mm diameter and 1000 mm length from TC Direct (Hillside, IL, USA) [18]. They were connected with 818-432-KX-type extension cables, twisted, shielded, and PVC insulated, with 724-102 and 724-104 K-type miniature connectors. In the experiments, the thermocouple stems were protected with an insulating sheet, as shown in Figure 4 for model 06 and analysed in Figure 5. The thermocouples were connected to a TC-08 thermocouple data logger from Pico Technology (Saint Neots, UK) [19]. The thermocouples were calibrated together with the numbered connecting cables through a Fluke 9142 (Fluke, Everett, WA, USA) RTD dry-block temperature analyser equipped with a PT100 probe [20]. The thermocouples were calibrated to 0.1 °C [20]. Even though the experiment was specifically designed for the casting was carried out in a sand foundry facility, a normal production, including the sand, forming equipment, air environment, and steel alloy. Prior to pouring, the temperature of the alloy was measured through a high-temperature probe, while an infrared thermometer gun measured all the materials in the experiment. These temperatures were registered and used in the subsequent phase of inverse optimisation to initialise the simulation temperatures.

2.3. Parameter Identification through Inverse Optimisation of Sand Properties

Parameter identification was carried out by means of inverse optimisation using the genetic algorithm (GA) technique. The GA sets different physical parameter values over a generation of GSC simulations. The results are evaluated by comparing these values to the experimental data. The parameters of the next generation are defined by merging the ones from the simulations with the lowest difference between real data and simulation results. Generation after generation, the GA identifies a set of parameters that best fit the experimental data. In this research, Magmasoft's Optimization Perspective module was used [16].

Simulation model 07 was used for this parameter identification step by reusing the standard HTC values as already described in Section 2.1. Since the heat resistance due to the solid mould is much higher, the error introduced with the standard HTC values is very little relevant to the identified properties of the sand. The first inverse optimisation identified six design variables for sand and cycle time:

- 1: the density of silica dry sand is constant, varying in the range of 1000–3000 kg/m^3, with steps of 10 kg/m^3; the preliminary evaluations described in Section 2.1 used the standard value of 1520 kg/m^3 from the Magmasoft database.
- 2 and 3: thermal conductivity is a two-step function that varies in the range of 0.1–1.5 W/mK, with steps of 0.05 W/mK at 20 °C, and again in the range of 0.1–1.5 W/mK, with steps of 0.05 W/mK, at temperatures above 500 °C; Figure 6 compares the variation function for thermal conductivity to the standard curve for silica dry sand, where the x-coordinates of the points to be identified are highlighted with black dashed lines.
- 4 and 5: specific heat capacity is a two-step function, varying in the range of 500–1000 J/kgK, with steps of 5 J/kgK at 20 °C, and in the range of 750–1750 J/kgK, with steps of 5 J/kgK at temperatures above 580 °C; Figure 7 compares the variation function for specific heat capacity to the standard curve for silica dry sand, where the x-coordinates of the points to be identified are highlighted with black dashed lines.
- 6: the start time is a constant parameter, varying in the range of 0–20 s, with steps of 1 s. The start time is used to account for possible errors in the synchronisation between the experiment and the start of the acquisition and also to model a delay in heat transfer to replace the neglected casting phase in the simulation model 07.

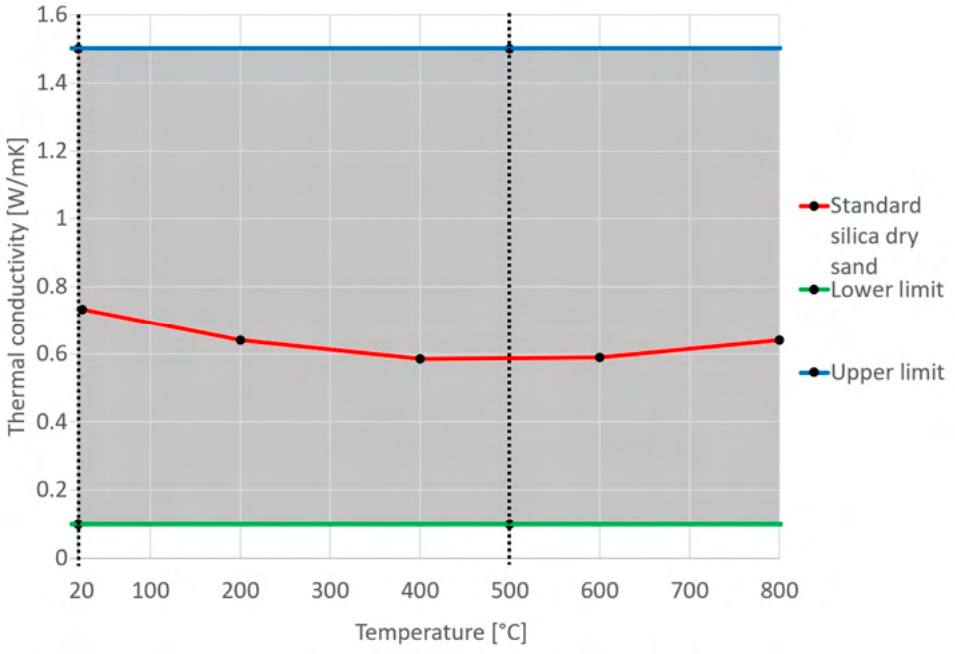

Figure 6. Variation of thermal conductivity in the inverse optimisation compared to the standard database function of silica dry sand.

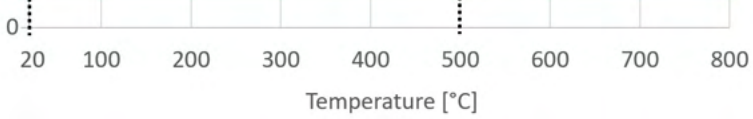

Figure 6. Variation of thermal conductivity in the inverse optimisation compared to the standard database function of silica dry sand.

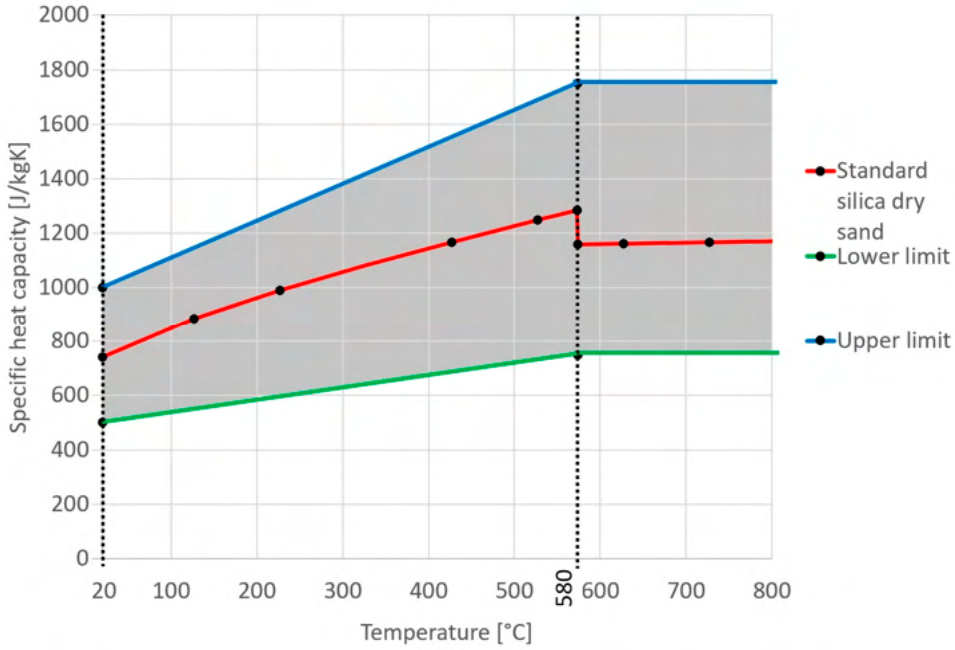

Figure 7. Variation in specific heat capacity for inverse optimisation compared to the standard database function of silica dry sand.

2.4. Parameter Identification through Inverse Optimisation of Heat Transfer Coefficients

This second inverse optimisation reused the model 07 adjusted with the identified parameters for sand density, thermal conductivity, and specific heat capacity, and identified three design variables for heat transfer between alloy and sand moulds for cycle time:

- 1 and 2: the HTC parametric function depends on the temperature of the contacting alloy, varying in the range of 200–1000 W/m^{2}K below the solidus temperature of 479 °C for AlSi9Cu1Mg, with steps of 10 W/m^{2}K, and in the range 500–2000 W/m^{2}K, with steps of 5 W/m^{2}K, at temperatures above the solidus temperature of 578 °C; Figure 8 compares the HTC variation function to the standard curve used for the Al alloy–sand pair, where the x-coordinates of the points to be identified are highlighted with black dashed lines;
- 3: the start time is a constant parameter, varying in the range 0–20 s, with steps of 1 s, with the function already described in the previous optimisation.

The optimisation was set again with the same measured data and objective function. The total number of different genotype combinations is 256,851. 15 generations with 8 designs each were calculated, for a total of 120 designs.

2.4. Parameter Identification through Inverse Optimisation of Heat Transfer Coefficients

This second inverse optimisation reused the model 07 adjusted with the identified parameters for sand density, thermal conductivity, and specific heat capacity, and identified three design variables for heat transfer between alloy and sand moulds for cycle time:

- 1 and 2: the HTC parametric function depends on the temperature of the contacting alloy, varying in the range of 200–1000 W/m^{2}K below the solidus temperature of 479 °C for AlSi9Cu1Mg, with steps of 10 W/m^{2}K, and in the range 500–2000 W/m^{2}K, with steps of 5 W/m^{2}K, at temperatures above the solidus temperature of 578 °C; Figure 8 compares the HTC variation function to the standard curve used for the Al alloy–sand pair, where the x-coordinates of the points to be identified are highlighted with black dashed lines;
- 3: the start time is a constant parameter, varying in the range 0–20 s, with steps of 1 s, with the function already described in the previous optimisation.

The optimisation was set again with the same measured data and objective function. The total number of different genotype combinations is 256,851. 15 generations with 8 designs each were calculated, for a total of 120 designs.

black dashed lines;

- 3: the start time is a constant parameter, varying in the range 0–20 s, with steps of 1 s, with the function already described in the previous optimisation.

The optimisation was set again with the same measured data and objective function. The total number of different genotype combinations is 256,851. 15 generations with 8 designs each were calculated, for a total of 120 designs.

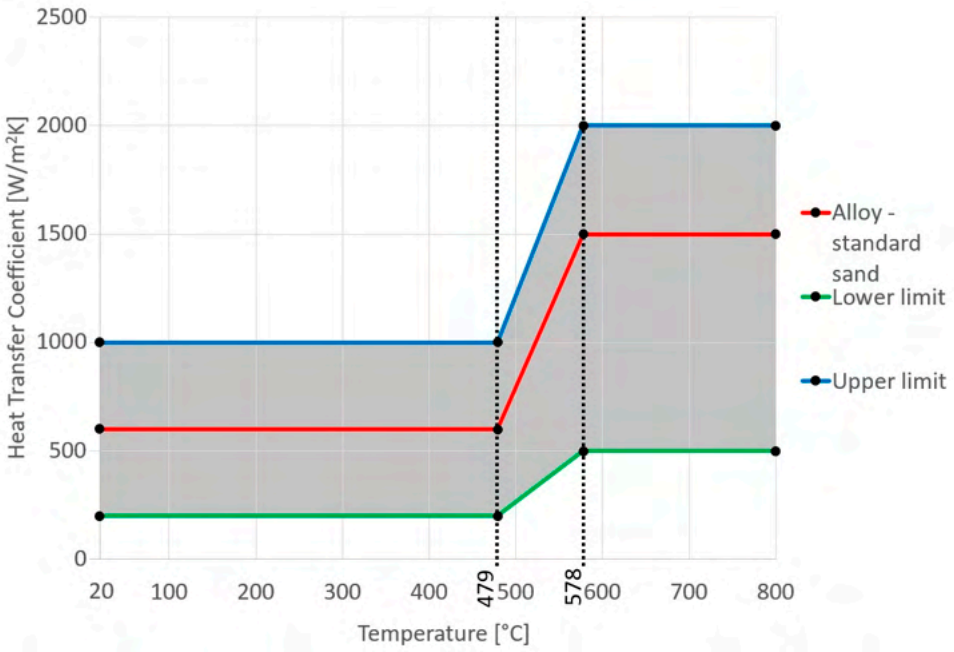

Figure 8. Variation in heat transfer coefficient in the inverse optimisation compared to the standard database function for the Al-alloy–sand pair.

3. Identification of Sand Thermal Parameters

3.1. Experiments with Virgin and Reused Silica Sand

The virgin sand is used in the foundry to create the cavity of the moulds and form the first thick layers, while the rest of the frame is filled with reused sand to save costs. Figure 9 shows a sample mould in which the thick layers close to the parting surface are formed with pale virgin sand while the rest is formed with a darker reused one. Virgin sand is used for the first layer as it offers consistent quality in the castings since it produces much less gas than reused sand. Nevertheless, it is also important to study the properties of cities of the reused sand in contact with the casting surfaces, as it can be used for the whole mould when it does not create quality problems.

Machines 2024, 12, x FOR PEER REVIEW

Figure 9. Sample mould in normal production with the layers close to the parting surface, the cavity inside formed with virgin sand, and the rest filled with reused sand.

Figure 9. Sample mould in normal production with the layers close to the parting surface, the cavity inside formed with virgin sand, and the rest filled with reused sand.

The used sand is always reused. After grinding, the sand is mechanically sifted to throw away dust with particles smaller than 70 µm. Most of the sand is therefore simply reconditioned with additional binder and reused in the process. Only part of it is further heat-treated to extract the resin and restore its virgin properties. The physical properties of the tested sands used to form the moulds are reported in Table 1. The physical analysis presented in Table 1 indicates noticeable differences, potentially attributed to the presence

The used sand is always reused. After grinding, the sand is mechanically sifted to throw away dust with particles smaller than 70 µm. Most of the sand is therefore simply reconditioned with additional binder and reused in the process. Only part of it is further heat-treated to extract the resin and restore its virgin properties. The physical properties of the tested sands used to form the moulds are reported in Table 1. The physical analysis presented in Table 1 indicates noticeable differences, potentially attributed to the presence of burned binder particles in the reused sand.

Table 1. Physical analysis of the tested sands.

Test	Standard	Virgin Silica Sand	Reused Silica Sand
Humidity [%]	B.PU.25 TV	0.10%	0.23%
Loss of calcination [%]	B.PU.12 TV	>10%	1.28%
Acid requirement (pH = 7) [ml HCl 0.1 N]	B.PU.01 SN	3.5	3.2
Sieve residue (fraction d $\leq$ 90 µm) [%]	B.PU.01 TV	0.19%	0.79%
Fineness index [-]	-	47	49

The first experiments were carried out with virgin silica sand, with each experiment performed in triplicate to ensure simulation reliability and validation. The temperature curves obtained in these experiments from the three thermocouples are illustrated in Figure 10. The first subscript represents the number of experimental replicas, resulting in the T_{1*}, T_{2*}, and T_{3*} curves. The second subscript represents the value recorded as T_{*1} curves for the thermocouple closest to the casting, T_{*2} for the central one, and T_{*3} for the farthest one. The temperature curves were averaged to upload the experimental data for the three thermocouples to Magmasoft. On average, the AlSi9Cu1Mg alloy was measured just before pouring at 719 °C, while the steel frame was at 31.2 °C and the sand mould at 27.7 °C.

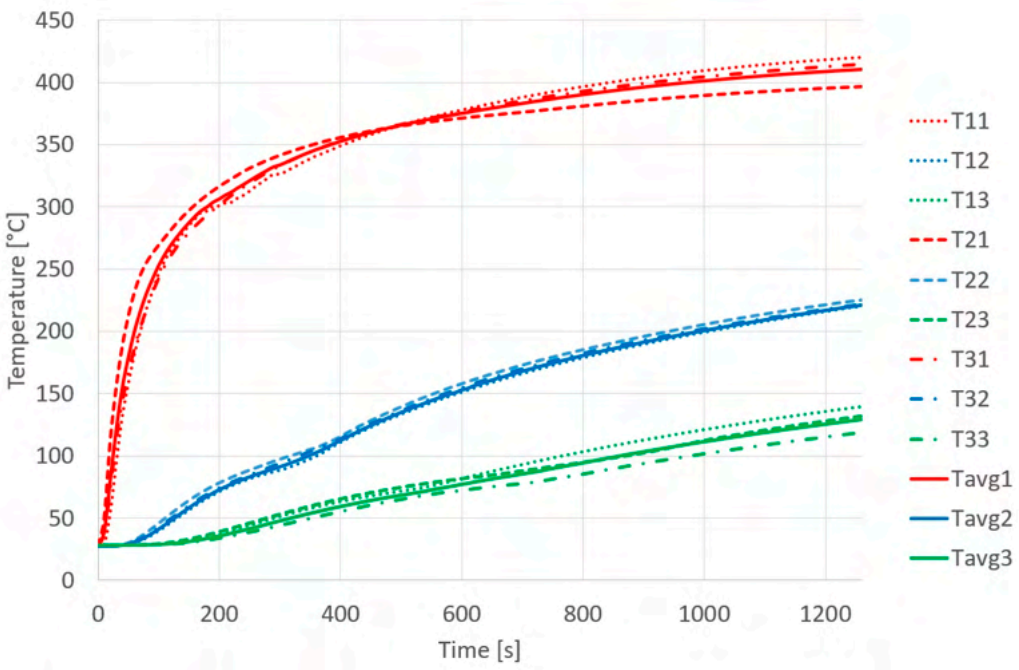

Figure 10. Temperature curves in the experiments with moulds formed from virgin silica sand.

Figure 10. Temperature curves in the experiments with moulds formed from virgin silica sand.

The experiments were repeated on reused silica sand, resulting in the temperature curves shown in Figure 11. On average, the alloy was measured at 699 °C, while the steel frame was at 38.9 °C and the sand mould at 38.4 °C.

The experiments were repeated on reused silica sand, resulting in the temperature curves shown in Figure 11. On average, the alloy was measured at 699 °C, while the steel frame was at 38.9 °C and the sand mould at 38.4 °C.

Figure 10. Temperature curves in the experiments with moulds formed from virgin silica sand.

The experiments were repeated on reused silica sand, resulting in the temperature curves shown in Figure 11. On average, the alloy was measured at 699 °C, while the steel frame was at 38.9 °C and the sand mould at 38.4 °C.

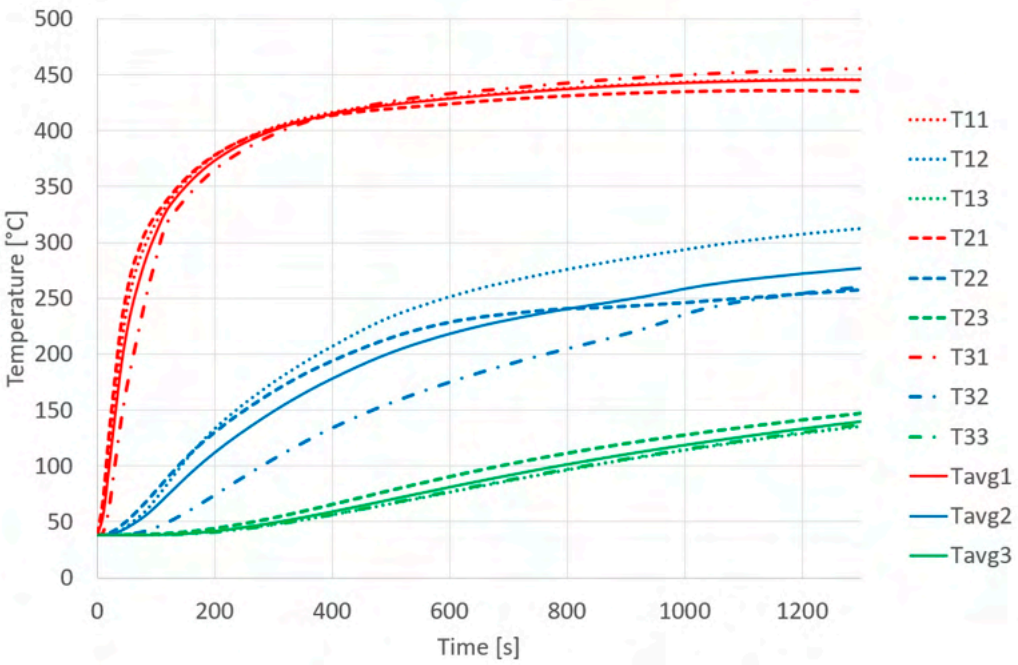

Figure 11. Temperature curves in the experiments with moulds formed from reused silica sand.

3.2. Identification of Sand Parameters

The first optimisation phase determined the density as 1570 kg/m^3 for virgin sand and 1560 kg/m^3 for reused sand, slightly higher than the 1520 kg/m^3 of the standard one. The identified thermal conductivities for virgin and reused sands, compared to the standard one, are reported in Figure 12. Figure 13 reports the specific heat capacities identified. For the thermal inertia of the system, the product of the aforementioned quantities is more important because it provides volumetric heat capacity, as shown in Figure 14. Finally, the start time was identified as 10 s for the experiment with virgin sand and 11 s for reused sand. The most important parameters for matching the measured and calculated curves include density, with a positive correlation of 0.25; the specific heat capacity level above 580 °C, with a correlation of −0.25; and the conductivity above 480 °C, with a correlation of 0.25. The correlation was low since many parameters interact while obtaining the objective function, justifying the use of the two-step identification method to converge the optimisation algorithm. The other parameters show negligible correlations in the experiments' temperature range. In particular, the negligible correlation with the objective start time demonstrates that the physical phenomenon is very slow. Therefore, simplifying the simulation without considering the pouring phase still provides reliable results.

3.3. Identification of Heat Transfer Parameters

The second optimisation identified HTCs, as shown in Figure 15. The standard curve for the HTC between Al alloy and sand is also reported. The most important parameter for matching the measured and calculated curves is the HTC level above a liquidus temperature of 578 °C, with a correlation of −0.75. Again, the closing time shows negligible correlation. The heat supplied by the casting before and during slow solidification is an important phenomenon.

of 0.25. The correlation was low since many parameters interact while obtaining the objective function, justifying the use of the two-step identification method to converge the optimisation algorithm. The other parameters show negligible correlations in the experiments' temperature range. In particular, the negligible correlation with the objective start time demonstrates that the physical phenomenon is very slow. Therefore, simplifying the simulation without considering the pouring phase still provides reliable results.

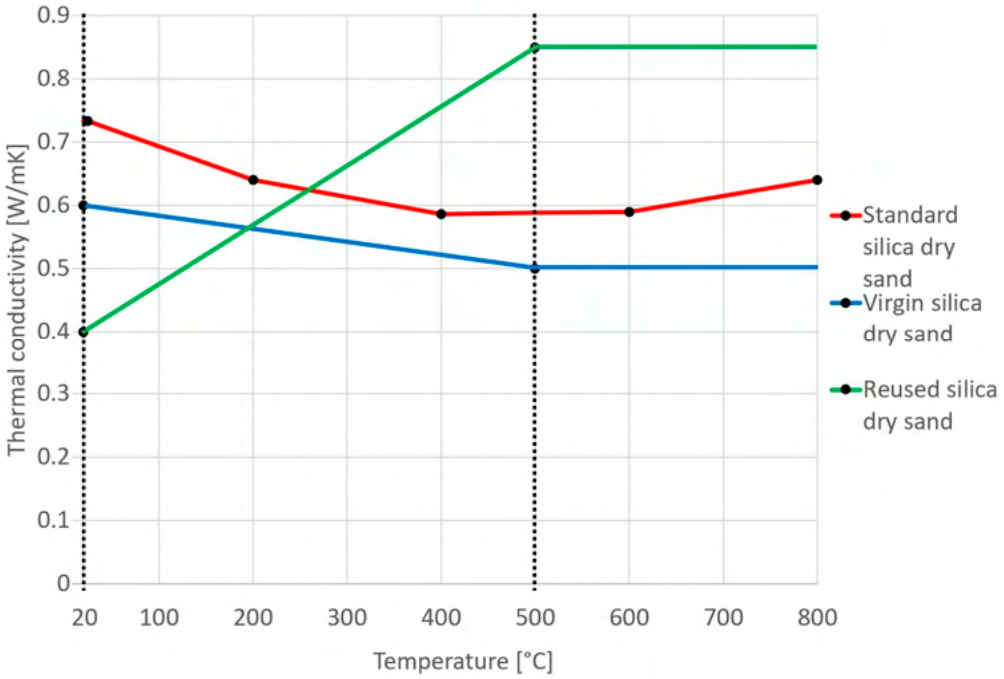

Figure 12. Thermal conductivity identified for virgin and reused sands compared to the standard curve from the database.

Figure 12. Thermal conductivity identified for virgin and reused sands compared to the standard curve from the database.

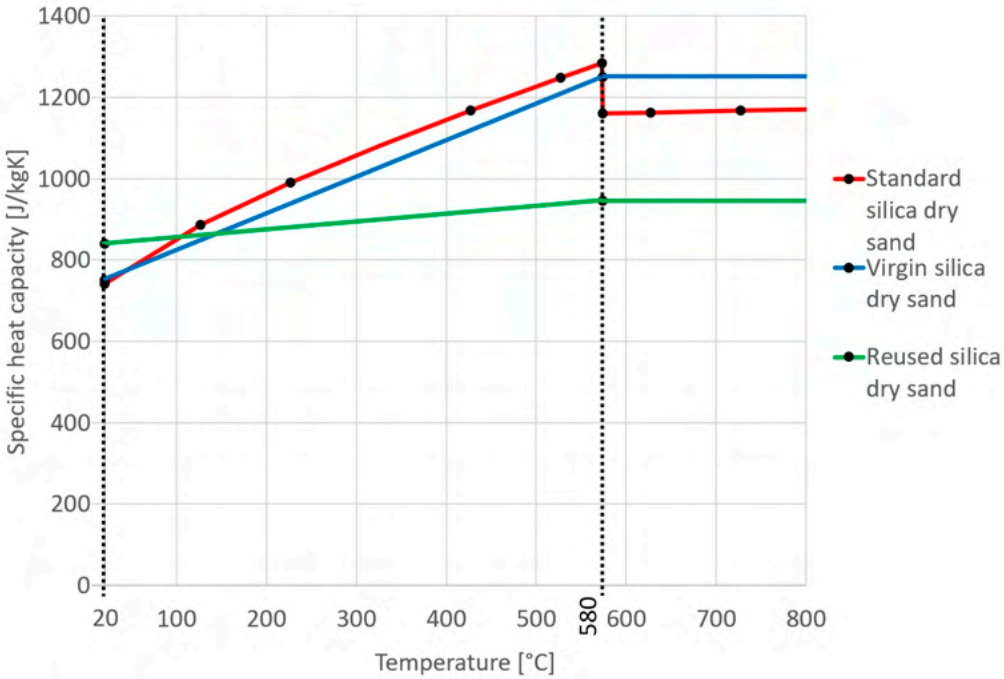

Figure 13. Specific heat capacity identified for virgin and reused sands compared with the standard curve from the database.

Figure 13. Specific heat capacity identified for virgin and reused sands compared with the standard curve from the database.

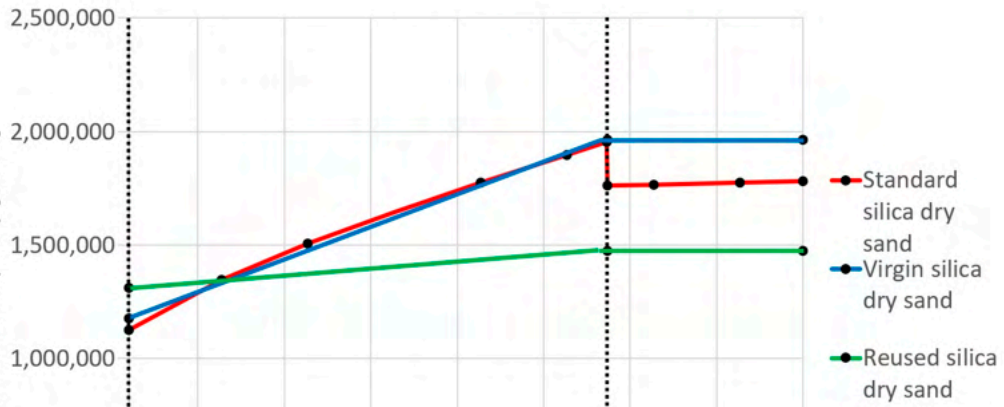

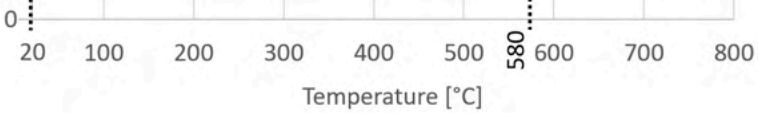

Figure 13. Specific heat capacity identified for virgin and reused sands compared with the standard curve from the database.

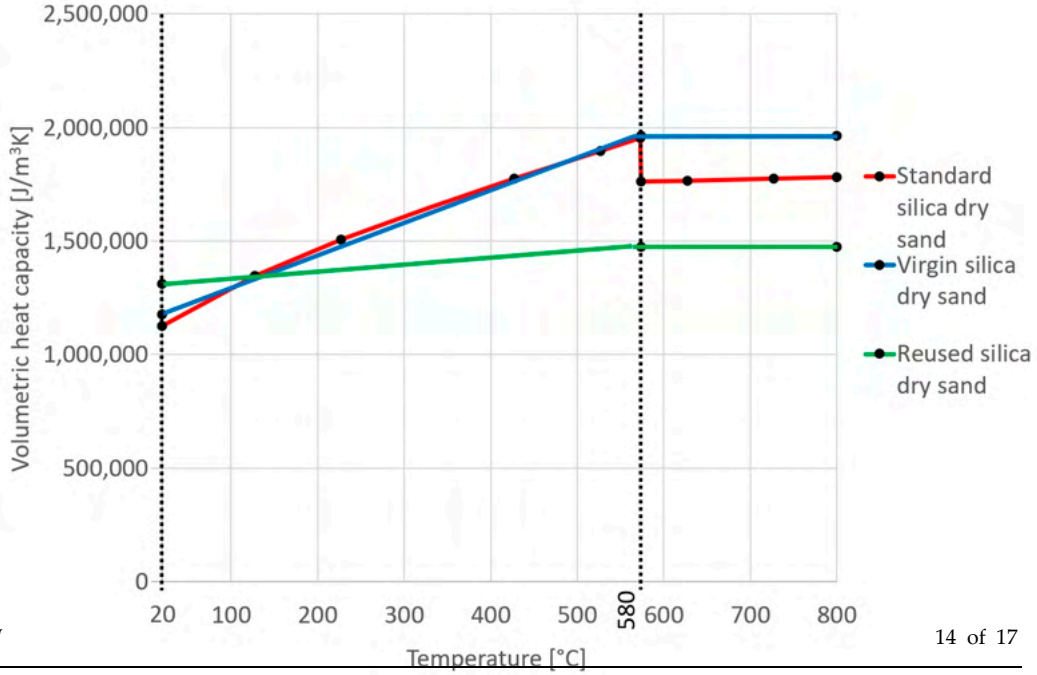

Figure 14. Curves calculated for the volumetric heat capacity of virgin and reused sands compared to the standard curve from the database.

The identified parameters for virgin and reused silica dry sand are reported in Table 2.

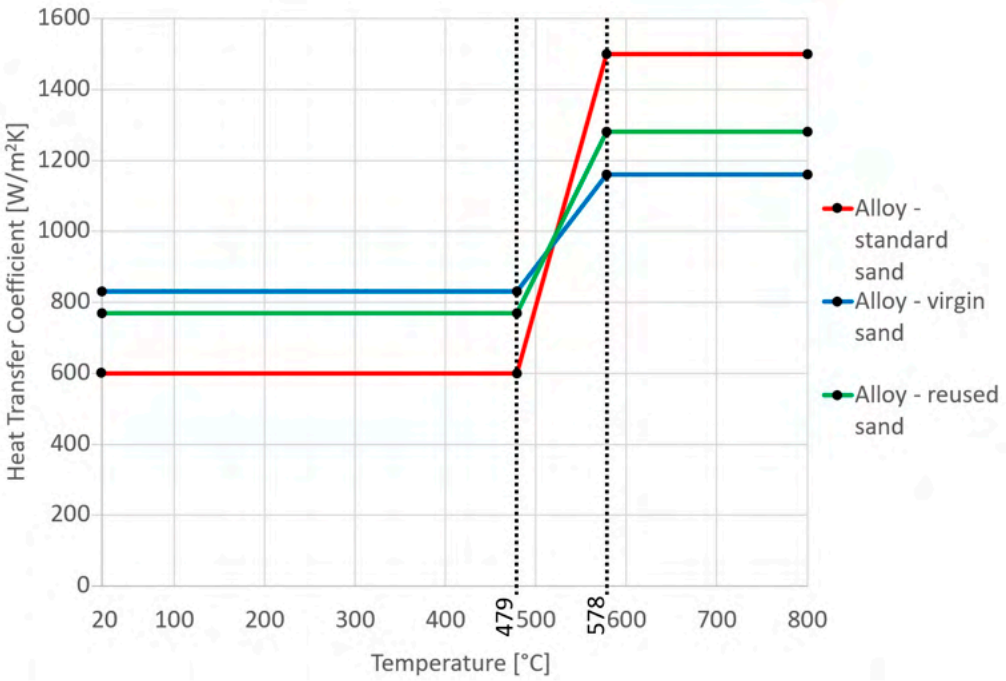

Figure 15. Identified HTCs for virgin and reused sands compared to the standard curve from the database.

Table 2. Identified parameters for virgin and reused silica dry sand and the HTC between AlSi9Cu1Mg alloy and sand.

Parameter	Virgin Silica Dry Sand [°C, Value]	Reused Silica Dry Sand [°C, Value]
Density [kg/m³]	any, 1570	any, 1560
Thermal conductivity [W/(m·K)]	20, 0.6 500, 0.5 800, 0.5	20, 0.4 500, 0.85 800, 0.85
Specific heat capacity [J/(kg·K)]	20, 750 580, 1250 800, 1250	20, 840 580, 945 800, 945
Volumetric Heat Capacity [J/(m³·K)]	20, 1,177,500 580, 1,962,500	20, 1,310,400 580, 1,474,200

Table 2. Identified parameters for virgin and reused silica dry sand and the HTC between AlSi9Cu1Mg alloy and sand.

Parameter	Virgin Silica Dry Sand [°C, Value]	Reused Silica Dry Sand [°C, Value]
Density [kg/m^3]	any, 1570	any, 1560
Thermal conductivity [W/(m·K)]	20, 0.6 500, 0.5 800, 0.5	20, 0.4 500, 0.85 800, 0.85
Specific heat capacity [J/(kg·K)]	20, 750 580, 1250 800, 1250	20, 840 580, 945 800, 945
Volumetric Heat Capacity [J/(m^3·K)]	20, 1,177,500 580, 1,962,500 800, 1,962,500	20, 1,310,400 580, 1,474,200 800, 1,474,200
HTC AlSi9Cu1Mg-sand [W/(m^2·K)]	20, 830 479, 830 578, 1160 800, 1160	20, 770 479, 770 578, 1280 800, 1280

3.4. Simulation with Standard and Identified Parameters

Final simulations were conducted on virgin and reused sand using the identified parameters. The simulated temperature curves using standard parameters from the database are compared in Figure 16a with the experiment with virgin sand and with the simulation using the parameters identified for it, while in Figure 16b they are compared with the experiment and simulation in the case of reused sand. Considering the difference between the actual and initial temperatures for each thermocouple as [(T1–T10), (T2–T20), (T3–T30)], that is, cancelling the variation due to different initial temperatures, the simulation with standard parameters results in average errors of [−0.91%, 4.52%, −4.49%] compared to experiments with virgin sand and in average errors of [−010.73%, −18.36%, 1.87%] compared to experiments with reused sand. The simulations using the parameters identified for sand resulted in average errors of [−0.84%, −0.74%, −3.44%] and [−2.05%, −8.42%, −3.07%] compared to experiments with virgin and reused sand, respectively.

for sand resulted in average errors of [−0.84%, −0.74%, −3.44%] and [−2.05%, −8.42%, −3.07%] compared to experiments with virgin and reused sand, respectively.

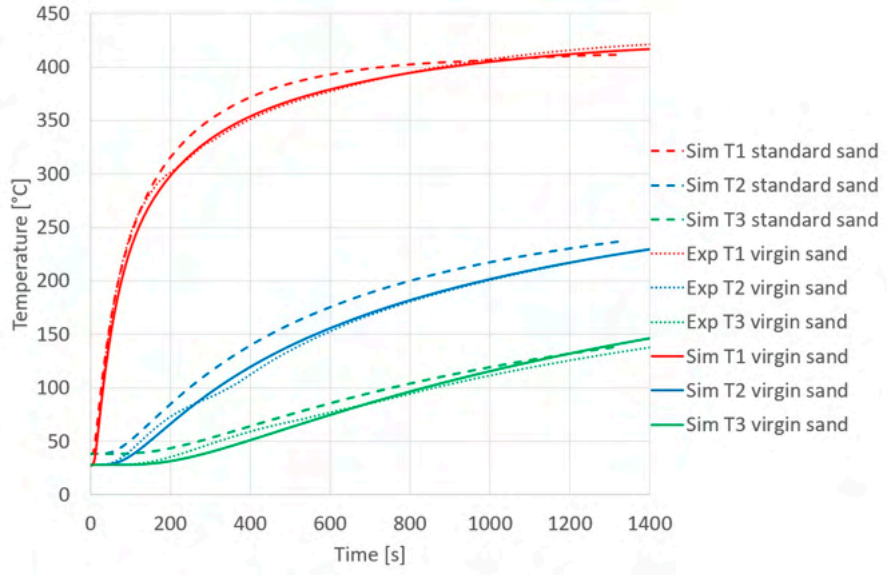

(**a**)

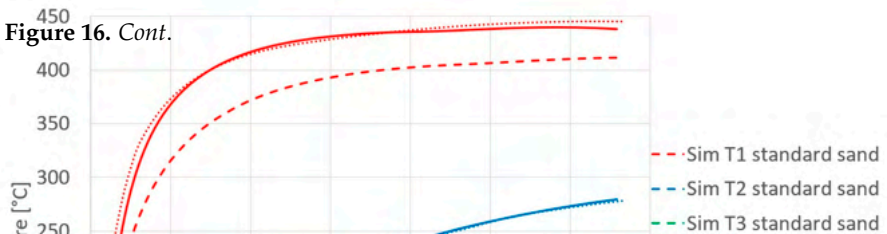

Figure 16. *Cont.*

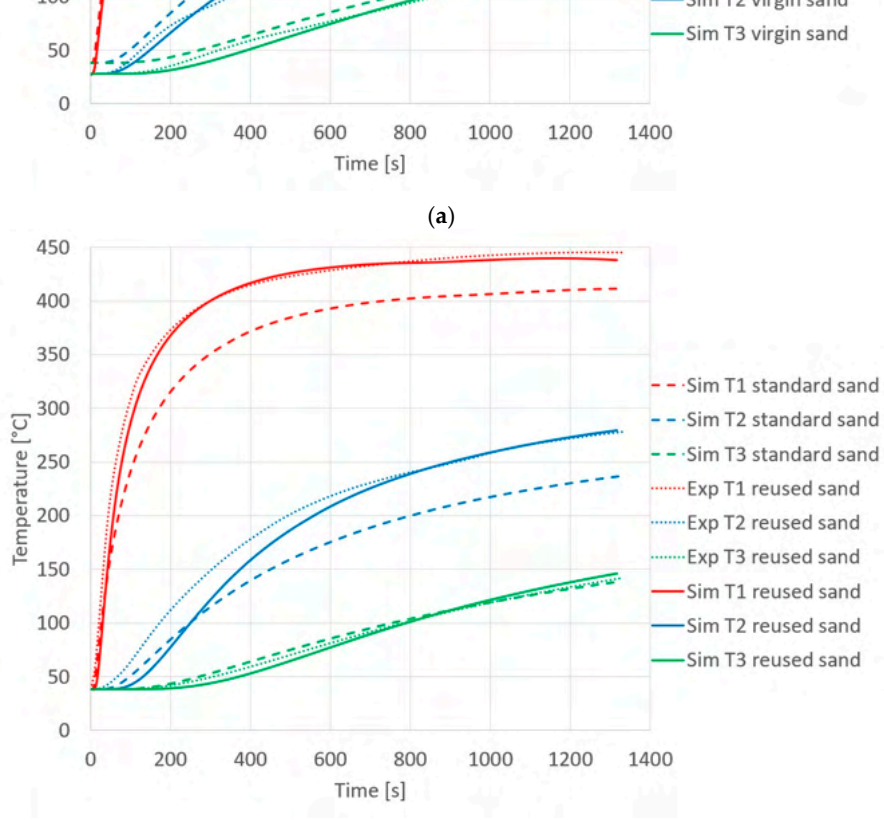

(**a**)

(**b**)

Figure 16. Comparison of the temperature curves calculated from simulation using standard parameters with the experimental and simulation curves for (**a**) virgin and (**b**) reused sands.

4. Conclusions

GA techniques were used in this study to identify the properties of the sand used to form moulds for GSC. This method was divided into two phases to reduce the number of parameters, thus allowing the GA to converge. In the first step, the sand properties were identified as temperature-dependent functions for density, thermal conductivity, and specific heat capacity. The volumetric heat capacity was determined by multiplying the density by the specific heat capacity. The HTC between the AlSi9Cu1Mg alloy and sand was also determined in a second identification step as a function of the alloy's liquidus and solidus temperatures. For the sake of computational efficiency, the simulation model only considered solidification without calculating the pouring of the melted alloy. It has been demonstrated that the elimination of the casting phase does not lead to a significant change in temperature trends. Considering this initial phase and any errors between the start of the experiment and the acquisition, the identification algorithm was also parameterised with a delay at the start of the experiment. However, the negligible correlation of these parameters with the objective function demonstrates that the simplification is reasonable with this slow heat transfer phenomenon.

The thermal parameters of the sand had greater relevance than the HTC in the evolution of the temperature field. Since the influence was greater, the sand parameters were identified more precisely.

The standard parameters proved to be quite reliable for virgin sand; however, they can still be improved as they vary depending on the preparation conditions in the foundry. In contrast, the standard parameters were not accurate for reused sand. As a result, the evolution of the temperature field may be different than expected, causing quality problems.

Ultimately, simulations conducted with the parameters identified for virgin and reused sands reproduced the temperature fields well.

Future work will involve designing equipment to measure sand parameters in the process, not as a tool to fine-tune the simulation but as a process control tool to predict the quality of the castings.

Author Contributions: Conceptualisation, A.V. and P.F.; methodology, validation, and simulation, A.V.; experiments, A.V. and P.F.; instrumentation and calibration, N.M.; data curation, A.V.; writing—original draft preparation, A.V. and N.M.; writing—review and editing, A.V., N.M., P.V., and F.L.;

supervision and project administration, P.V. and F.L.; funding acquisition, A.V. and P.F. All authors have read and agreed to the published version of the manuscript.

Funding: The authors declare that this study received funding from Fonderia Morri, Via A. Manzoni 7, 47853 Cerasolo, Italy. The funder had the following involvement with the study: conceptualisation, facilities, experiments.

Data Availability Statement: Raw data supporting the conclusions of this article will be made available by the authors upon request.

Acknowledgments: The authors are grateful to Fonderia Morri, Cerasolo, Italy, for their available facilities and technical support in setting up and running the experiments.

Conflicts of Interest: Author Pietro Facondini was employed by the company Fonderia Morri. The remaining authors declare that the research was conducted in the absence of any commercial or financial relationships that could be construed as a potential conflict of interest.

References

1. Khan, M.A.A.; Sheikh, A.K. A comparative study of simulation software for modelling metal casting processes. *Int. J. Simul. Model.* **2018**, *17*, 197–209. [CrossRef]
2. Ravi, B. Casting simulation and optimisation: Benefits, bottlenecks and best practices. *Indian. Foundry J.* **2008**, *54*, 47.
3. Vergnano, A.; Salvati, E.; Magistrelli, A.; Brambilla, E.; Veronesi, P.; Leali, F. A method for yield and cycle time improvements in Al alloy casting with enhanced conductivity steel for die construction. *Manuf. Rev.* **2022**, *9*, 9–18. [CrossRef]
4. Swain, M.V.; Johnson, L.F.; Syed, R.; Hasselman, D.P.H. Thermal diffusivity, heat capacity and thermal conductivity of porous partially stabilized zirconia. *J. Mater. Sci.* **1986**, *5*, 799–802. [CrossRef]
5. Nait-Ali, B.; Haberko, K.; Vesteghem, H.; Absi, J.; Smith, D.S. Thermal conductivity of highly porous zirconia. *J. Eur. Ceram. Soc.* **2006**, *26*, 3567–3574. [CrossRef]
6. Codorníu, D.M.; Moyano, J.J.; Belmonte, M.; Osendi, M.I.; Miranzo, P. Thermal conduction in three-dimensional printed porous samples by high resolution infrared thermography. *Open Ceram.* **2020**, *4*, 100028. [CrossRef]
7. Park, S.S.; Park, J.W.; Yoon, K.B.; Park, I.S.; Woo, S.W.; Lee, D.E. Evaluation of compressive strength and thermal conductivity of sand stabilized with epoxy emulsion and polymer solution. *Polym. J.* **2022**, *14*, 1964. [CrossRef]
8. Zhang, N.; Wang, Z. Review of soil thermal conductivity and predictive models. *Int. J. Therm. Sci.* **2017**, *117*, 172–183. [CrossRef]
9. Smith, D.S.; Alzina, A.; Bourret, J.; Nait-Ali, B.; Pennec, F.; Tessier-Doyen, N.; Otsu, K.; Matsubara, H.; Elser, P.; Gonzenbach, U.T. Thermal conductivity of porous materials. *J. Mater. Res.* **2013**, *28*, 2260–2272. [CrossRef]
10. Myers, A.L. Thermodynamics of adsorption in porous materials. *AIChE J.* **2002**, *48*, 145–160. [CrossRef]
11. Pedrazzi, S.; Vergnano, A.; Allesina, G.; Veronesi, P.; Leali, F.; Tartarini, P.; Muscio, A. A simple test method for measurement of the interface thermal resistance of coated and uncoated metal surfaces. *J. Phys. Conf. Ser.* **2020**, *1599*, 012049. [CrossRef]
12. Pagratis, N.; Karagiannis, N.; Vosniakos, G.-C.; Pantelis, D.; Benardos, P. A holistic approach to the exploitation of simulation in solid investment casting. *Proc. Inst. Mech. Eng. Pt. B J. Eng. Manufact* **2007**, *221*, 967–979. [CrossRef]
13. Guo, Z.-P.; Xiong, S.-M.; Liu, B.C.; Li, M.; Allison, J. Determination of the metal/die interfacial heat transfer coefficient and its application in evaluating the pressure distribution inside the casting during the high pressure die casting process. *Int. J. Cast. Met. Res.* **2009**, *22*, 327–330. [CrossRef]
14. Vasileiou, A.N.; Vosniakos, G.C.; Pantelis, D.I. On the feasibility of determining the heat transfer coefficient in casting simulations by genetic algorithms. *Procedia Manuf.* **2017**, *11*, 509–516. [CrossRef]
15. Zhang, L.; Li, L.; Ju, H.; Zhu, B. Inverse identification of interfacial heat transfer coefficient between the casting and metal mold using neural network. *Energy Convers. Manag.* **2010**, *51*, 1898–1904. [CrossRef]
16. Magmasoft. MAGMASOFT Autonomous Engineering. Available online: https://www.magmasoft.de/en/ (accessed on 22 May 2024).
17. MONALITE Insulating Panels, Promat SpA. Available online: https://www.promat.com/it-it/industry/prodotti-soluzioni/isolamento-ad-alta-temperatura/lastre-hti/monalite/ (accessed on 17 April 2024).
18. TC Direct. Available online: https://www.tcdirect.it (accessed on 15 April 2024).
19. Pico Technolgy LTD, Tc-08 Datasheet. 2021. Available online: https://www.picotech.com/data-logger/tc-08/usb-tc-08-manuals (accessed on 15 April 2024).
20. Franco Corradi Apparecchiature per Industrie e Laboratori, Temperature Analyzer with Platinum Resistance Thermometer, Model RP7000, Series No. 453/30. Franco Corradi Apparecchiature per Industrie e Laboratori. Available online: www.francocorradi.it (accessed on 7 June 2024).
21. Haupt, R.L.; Haupt, S.E. *Practical Genetic Algorithms*; John Wiley & Sons: Hoboken, NJ, USA, 2004; pp. 127–135.